Improved Bearing Estimates of Weak Signals Using Stochastic Resonance and Frequency Shift Techniques

Qinghua Ye*, Haining Huang**, Xinyi He and Chunhua Zhang
Institute of Acoustics, Chinese Academy of Sciences
21 Beisihuanxi Street, Haidian, Beijing 100080, China
Email: *qhye@sina.com, **drhhn@263.net

***Abstract*-This paper presents a method to estimate bearings of weak signals using stochastic resonance (SR) and frequency shift techniques. After the signals received from the array sensors are translated to baseband and filtered by a stochastic resonator, the signal-to-noise ratio can be greatly enhanced. Higher performance for the beamforming output is obtained using the proposed method, comparing to the conventional beamforming result.**

I. INTRODUCTION

Conventional sonar systems are annoyed by the background noise. When the noise is heavy, the bearing estimate methods such as the conventional beamforming (CBF) are not so effective. Under certain circumstances, however, an extra dose of noise can in fact help rather than hinder the performance of the bearing estimate, and this led us to investigate a stochastic resonance (SR) based method to estimate the bearings of signals under very low signal-to-noise ratio (SNR). In previous work [1], a stochastic resonator was used directly on the receiving signal sequence for each array sensor to enhance the weak periodic signal. This previous method works well when the signal frequency is low, but if the signal frequency is high, the signal amplification effect may be weakened. In this paper, we discuss the stochastic resonance for very low frequency signal and develop the previous method by translate the received signal to baseband in frequency domain beamforming. As a consequence, high frequency weak signal can also be enhanced and we can obtain good bearing estimate from the beamforming output.

In our processing scheme, signals sampled from a linear array are first decomposed into different narrowband signals (demodulated and low pass filtered) using FFT [2,3]. Secondly, the narrowband signal for each sensor of the array in each frequency subband is processed by a stochastic resonator to enhance the weak signal. Thirdly, the output signals from the stochastic resonator for all sensors in each frequency subband are processed by the conventional beamforming method. In order to display the bearings of broadband signals, their energies are estimated and summed along each looking direction. For narrowband signals with known center frequency the above steps can be processed only on the desired few subbands and then the computational requirement decreases.

II. STOCHASTIC RESONANCE

The term stochastic resonance (SR) is given to a phenomenon that appears in nonlinear systems whereby the addition of noise to a system enhances its response to a periodic force [4-6]. The effect requires three basic ingredients: a form of threshold, a source of "noise," and a generally weak input source [5].

We consider an overdamped motion of a Brownian particle in a bistable potential in the presence of noise and periodic forcing [5]

$$\dot{x}(t) = -V'(x) + A_0 \cos(\Omega t + \varphi) + \xi(t), \qquad (2.1)$$

where A_0 is the signal amplitude and Ω is the modulation frequency. Here, we assume that the noise $\xi(t)$ is zero-mean, Gaussian white noise with an autocorrelation function given by $\langle \xi(t)\xi(0)\rangle = 2D\delta(t)$. $V(x)$ denotes a symmetric bistable potential $V(x) = -\frac{a}{2}x^2 + \frac{b}{4}x^4$. The potential minimas are located at $\pm x_m$, with $x_m = \sqrt{a/b}$. The height of the potential barrier between the two minimas is $\Delta V = \frac{a^2}{4b}$.

In the absence of periodic forcing, $x(t)$ fluctuates around its local stable states. Noise-driven switching between the local equilibrium states occurs at the Kramers rate [5,6]

$$r_k = \frac{a}{\sqrt{2}\pi}\exp\left(-\frac{\Delta V}{D}\right). \qquad (2.2)$$

When we apply a weak periodic forcing to the particle, noise-driven switching between the potential wells can become synchronized with the weak periodic forcing. This statistical synchronization takes place when the average waiting time $T_K(D) = 1/r_K$ between two noise-driven interwell transitions satisfies the time-scale matching condition, i.e.,

$$2T_K(D) = T_\Omega, \qquad (2.3)$$

where T_Ω is the period of the periodic forcing [5].

For convenience, we choose the initial phase of the periodic driving $\varphi = 0$. When $t \to +\infty$, the memory of the initial conditions gets lost and the mean value $\langle x(t)\rangle_{as}$ becomes a periodic function of time, i.e., $\langle x(t)\rangle_{as} = \langle x(t+T_\Omega)\rangle_{as}$. For small amplitudes, the response of the system to the periodic input signal can be written as [5]

$$\langle x(t)\rangle_{as} = \bar{x}\cos(\Omega t - \bar{\phi}), \qquad (2.4)$$

with amplitude $\bar{x}$ and a phase lag $\bar{\phi}$. Approximate expressions for $\bar{x}$ and $\bar{\phi}$ are

$$\bar{x}(D) = \frac{A_0\langle x^2\rangle_0}{D}\frac{2r_K}{\sqrt{4r_K^2+\Omega^2}}, \qquad (2.5)$$

and

$$\bar{\phi}(D) = \arctan\left(\frac{\Omega}{2r_K}\right), \tag{2.6}$$

where $\langle x^2 \rangle_0$ is the D-dependent variance of the stationary unperturbed system ($A_0 = 0$). Equation (2.5) has been shown to hold in leading order of the modulation amplitude $A_0 x_m / D$ for both discrete and continuous one-dimensional systems, i.e. $\langle x^2 \rangle_0 = x_m^2$.

The above (2.5) and (2.6) show that the phase of the output signal is consistent with the input signal, while exhibits a phase lag $\bar{\phi}$. When using SR in array signal processing, the phase lag for each sensor is the same, providing the applicability of using SR in array signal processing.

A. Discrete time implementation

We use a discrete computer simulation with the stochastic version of Euler's method (the Euler-Maruyama scheme [6])

$$x_{n+1} = x_n + \Delta T(ax_n - bx_n^3 + u_n), \tag{2.7}$$

with initial condition $x_0 = x(0)$. Here u_n is the input time sequence. The process's sampling period T_s can differ from the time step ΔT in (2.7).

B. Stochastic resonance for very low frequency signals

The behavior of SR depends on the signal amplitude A, signal frequency Ω and noise intensity *D*. Fig. 1 is the output SNR as a function of signal frequency Ω and noise intensity *D* when the parameters in (2.7) are $a=1$, $b=1$ at a fixed signal amplitude A_0. We observe that for a fixed signal amplitude A_0 and a fixed noise intensity the stochastic resonance behavior of the output SNR decreases upon increasing the signal frequency Ω. When the input signal is a DC signal as an extreme case, the "resonance" effect of SR disappears, i.e. the output SNR decreases upon increasing the noise intensity with fixed signal amplitude A_0, but otherwise the output SNR is better than that when the input is a sinusoid signal.

In array processing by moving a high frequency signal to baseband then through a stochastic resonator the signal can be enhanced effectively, and we get improved bearing estimates not only for low frequency signals but for high frequency ones.

III. BEARING ESTIMATES USING STOCHASTIC RESONANCE

Broadband beamforming can be implemented in either time or frequency domain. We employ in this paper the frequency domain beamformer. In a frequency domain beamformer, the broadband signal is decomposed into multiple narrowband signals. Phase shift is used to make the signals arriving from the looking direction coherent at the outputs of all sensors for each subband [2,3].

For *N* sensors of a beamformer, plane-wave steering vectors are defined as in (3.1) for a uniformly spaced linear array

$$\mathbf{s}(\theta) = \begin{bmatrix} 1 & e^{-j2\pi f \frac{D\sin\theta}{C}} & \cdots & e^{-j2\pi f \frac{(N-1)D\sin\theta}{C}} \end{bmatrix}^T. \tag{3.1}$$

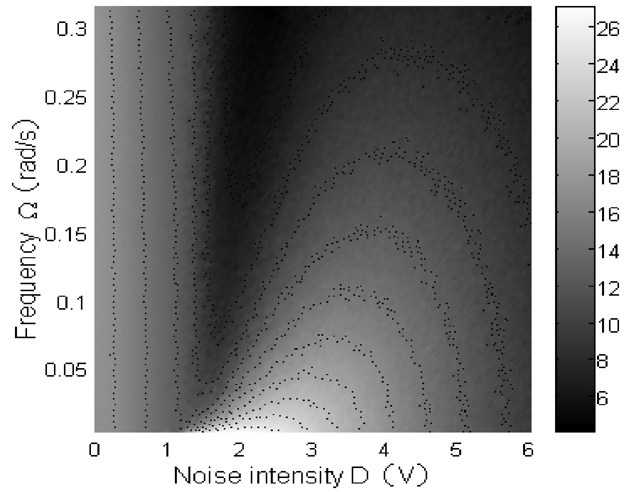

Fig. 1. Output *SNR* as a function of signal frequency Ω and noise intensity *D* when $a = 1, b = 1$.

In this equation, *f* is the subband center frequency, *D* is the distance between sensors, *C* is the speed of sound, and θ is the steering direction. The output of the beamformer is expressed by

$$y(t) = \mathbf{s}(\theta)^H \cdot \mathbf{x}(t), \tag{3.2}$$

where $\mathbf{s}(\theta)$ is the steering vector defined in (3.1), $\mathbf{x}(t)$ is the vector of the Fourier component of received data near the processing frequency, and operator *H* represents complex conjugation and matrix transposition. The output spectral density of the beamformer is then given by

$$P(\theta) = E[|y(t)|^2] = \mathbf{s}(\theta)^H \cdot \mathbf{R} \cdot \mathbf{s}(\theta), \tag{3.3}$$

where **R** is the cross-spectral matrix, $\mathbf{R} = E[\mathbf{x}(t)^H \cdot \mathbf{x}(t)]$.

To enhance weak signals from the received data, we translate the data to baseband and filter them by a stochastic resonator before beamforming. The major steps of our approach are discussed below in detail. The signal decomposition (section A) was described in [2]. For narrowband signals with known center frequency the following steps can be processed only on the desired few subbands and then the computational requirement decreases.

A. Signal Decomposition

Signals received from array sensors subdivided into subbands. Each subband is then translated to baseband through complex demodulation (i.e. the center frequency of the subband is moved to 0 Hz). Subsequently, using a low pass filter with very narrow bandwidth, signals and noises outside the subband are removed. The band shifting and filtering are performed on consecutive subbands. For the sampled sequence, $x_m(n)$, derived from the *m*th element, the output signal of the ith subband filter, $x_{m,i}(n)$, can be expressed by

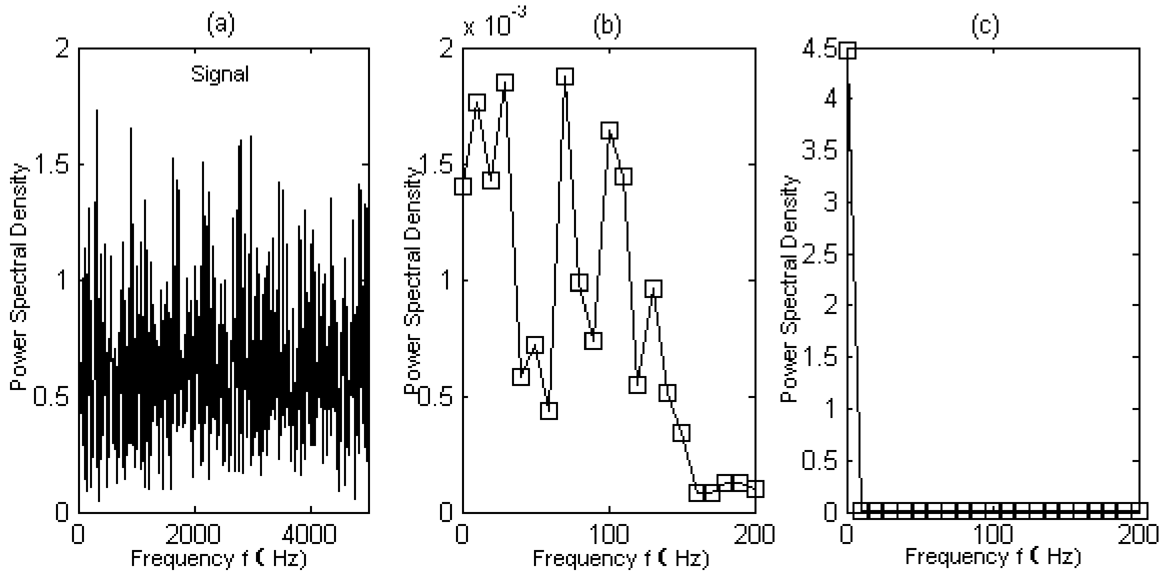

Fig. 2. Power spectral density of the following signals: (a) The 33*th* subband corresponding to signal frequency from one of the sensor; (b) the baseband signal; (c) signal passed the stochastic resonator.

$$x_{m,i}(n)=\sum_{l=0}^{L-1}h_L(l)x_m(n-l)e^{-j\omega_i(n-l)}, \tag{3.4}$$

where L is the length of FIR filter h_L. A reshaped form of the output signal is

$$x_{m,i}(n)=e^{-j\omega_i n}\sum_{l=0}^{L-1}h_L(l)x_m(n-l)e^{-j\omega_i l}. \tag{3.5}$$

The demodulating frequency ω_i is chosen to be $\omega_i=2\pi i/L$ so that the demodulation and summation operations in the above equation can be implemented using FFT (with a record length L) preceded by the data windowing h_L.

B. Filtering by SR

The normalized output signal of the ith subband $x_{m,i}'(n)$, derived from the mth sensor, is filtered by a stochastic resonator using (2.7)

$$y_{m,i}(n+1)=y_{m,i}(n)+\Delta T[ay_{m,i}(n)-by_{m,i}^{3}(n)+x_{m,i}'(n)]. \tag{3.6}$$

Here $y_{m,i}(n)$ is the output signal from the stochastic resonator, and $x_{m,i}'(n)=x_{m,i}(n)/\max(|x_{m,i}|)$ then $x_{m,i}'(n)\in[-1,1]$. The parameters in the above equation we used are $\Delta T=0.0195$, $a=0.1$, $b=0.01$. They were determined experimentally.

C. Spatial covariance estimation and beamforming

The estimate of covariance matrix in (3.3) is obtained by

$$\hat{\mathbf{R}}_i=\frac{1}{K}\sum_{k=1}^{K}\mathbf{y}_i(k)\mathbf{y}_i^H(k), \tag{3.7}$$

where the subscript i represents the ith subband. In our experiment, $\hat{\mathbf{R}}_i$ is updated for every snapshot. The covariance estimation is performed for each of the subbands.

Beams in 0-180° azimuth angle are formed for each subbands, then beam output energy is computed. Power sum is employed to combine the subband results.

IV. SIMULATION RESULTS

In our simulation, we used a linear array consisting of 8 sensors with a source at $\theta=30°$ with the SNR –30dB (zero-mean, Gaussian white noise). The signal and sampling frequency are 1.25 and 10 kHz respectively. Using a 256 point FFT, there are 128 samples in either the upper or the lower sideband. Each sample represents one subband. Only either one of these two sidebands is required.

The 33*th* subband (corresponding to signal frequency) from one of the sensor is translated to baseband through complex demodulation and passes a low pass filter using (3.5). The order of the low pass filter h_L is 255 with a stop frequency 200 Hz. The power spectral density (PSD) of the 33*th* subband signal and its baseband are depicted in Fig. 2(a) and Fig. 2(b). Because of the low SNR, the PSD of the signal frequency (1250 and 0 Hz respectively) can't be recognized.

Fig. 2(c) is the PSD after the baseband signal passes the stochastic resonator. With the enhanced SNR, the PSD at frequency of 0 Hz is prominent.

Fig. 3 is the normalized output of conventional beamforming. The dashed line is the beamforming output not through the stochastic resonantor, and the solid line is the beamforming output through the stochastic resonator. From Fig. 3 we can see that the proposed method is capable of estimating the bearings of signals under low signal-to-noise ratio. Comparing to our previous work [1], the method presented in this paper can deal with high frequency signals without the high sampling frequency restriction.

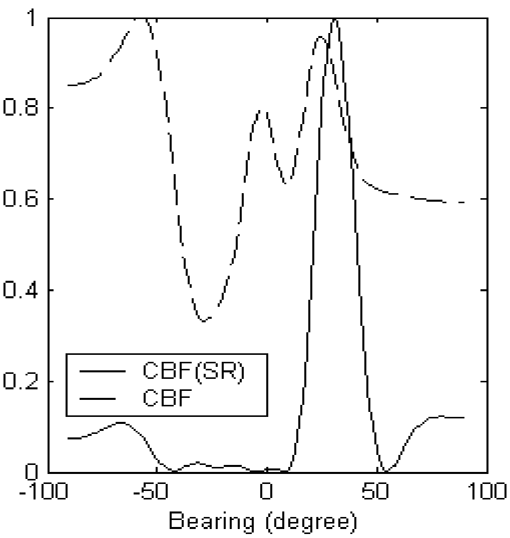

Fig. 3. Normalized output of conventional beamforming. The dashed line is the beamforming output not through SR, and the solid line is the beamforming output through SR.

V. CONCLUSION

This paper uses a property of a SR system that differs from the common definition of SR. This property is that a SR system can accumulate and amplify the energy of a very low frequency (especially a direct current) weak signal. By translation the signals received from the array to baseband and filtering them by a stochastic resonator, the SNR can be greatly enhanced. In our simulations higher performance for the beamforming output is obtained using the proposed method, comparing to the conventional beamforming output. The results show that SR is a potential useful tool for underwater signal processing and array signal processing. Real data tests are required in our following work.

REFERENCES

[1] Q. Ye, H. Huang, X. He and C. Zhang, "DOA estimation of weak signals via stochastic resonance ," *Chinese Journal of Acoustics*, in press (in Chinese).

[2] B. Kim and I. Lu, "High resolution broadband beamforming based on the MVDR method," *Proc. MTS/IEEE Oceans 2000*, vol.3, pp. 1673-1676, Sept 2000.

[3] R.O. Nielsen, *Sonar Signal Processing*, Artech House, Boston, London, 1991, pp. 84-91.

[4] K. Wiesenfeld, and F. Moss, "Stochastic resonance and the benefits of noise: from ice ages to crayfish and SQUIDs," *NATURE*, vol 373.5, pp. 33-36, 1995.

[5] L. Gammaitoni, P. Hanggi, P. Jung, and F. Marchesoni, "Stochastic resonance," *Reviews of Modern Physics*, vol. 70, No. 1, pp. 223-287, 1998.

[6] S. Mitaim, and B. Kosko, "Adaptive Stochastic Resonance," *PROCEEDINGS OF THE IEEE*, vol. 86, No. 11, pp. 2152-2183, 1998.